

Influence of Sulphur content on the optical properties of glassy S_xSe_{100-x} thin films system

M. M. EL NAHASS*, M. B. EL DEN^a, H. E. A. EL-SAYED, A. M. A. EL-BARRY, M. A. M. SEYAM

^aPhysics Department, Faculty of Science, Ain Shams University, Cairo, Egypt

Physics Department, Faculty of Education, Ain Shams University, Cairo, Egypt

Thin films of S_xSe_{100-x} , where $x = 0, 2.5, 5.8$ and 7.28 at % S, have been prepared by thermal evaporation technique using quartz and glass substrates kept at room temperature (300 K). EDX analysis of all the S_xSe_{100-x} compositions prepared indicate that the compositions are stoichiometric. X-ray diffraction patterns for S_xSe_{100-x} compositions, in powder form as well as in thin film forms have an amorphous nature for as deposited films and polycrystalline nature of hexagonal phase after being annealed at 423 K for one hour. DAT measurements gave three transition temperatures T_g , T_c and T_m . The optical constants were determined for films of different thickness values (100-500 nm) by using spectrophotometric measurements of the transmittance, T , and the reflectance, R , at normal incidence in the spectral range 400-2500 nm. The obtained values of both n and k were found to be independent of the film thickness. The refractive index, n , attains a peak value at wavelength λ_c , which is shifted towards the shorter wavelength as the sulphur content is increased. The estimated width of localized states in the forbidden gap and the variation of the indirect and direct optical energy gap as a function of both sulphur content and annealing temperature have been determined. The values of the dispersion energy E_d , the single oscillator energy E_0 , the infinite dielectric constant ϵ_{∞} , the lattice dielectric content ϵ_L and the ratio N/m^* , of the system have been determined and correlated with the type and amount of chemical bonds. The effect of heat treatment on the optical parameters have been also discussed.

(Received June 11, 2006; accepted September 13, 2006)

Keywords: Optical properties, Thin films, S_xSe_{100-x}

1. Introduction

Some chalcogenide glasses exhibit novel electrical and optical properties, such as switching and memory effects, and photo-darkening phenomenon [1-3] which allow them to be used for improved applications in electronic devices and photo-recording materials. Although most chalcogenide glasses reported to date for optical-recording media usually contain selenium or tellurium as a main constituent element [4,5]. Besides, sulphur-chalcogenides [6,7] were used in this field [7,9]. Studies of structure, phase transformation and composition dependence of the transport properties in S-Se chalcogenide compounds have been studied [8,9].

In the present work, the composition dependence of the optical parameters of the glassy system S_xSe_{100-x} with $x = 0, 2.5, 5$ and 7.28 at % S, have been studied at room temperature as well as after annealing at 433 K for 2 hours, and the results have been correlated with the concentration of sulphur.

2. Experimental technique

Four compositions of the system S_xSe_{1-x} with $x = 0, 2.5, 5$ and 7.28 at % S have been prepared by fusing high purity elements (99.99%) in appropriate weights in evacuated pyrex ampoules at 623 K for 3h. During synthesis the ampoules were shaken continuously to enable complete homogeneity of the ingots. After

synthesis, the molten was quenched in air. Before the preparation of the thin films, the amorphous nature and the homogeneity of the ingots were examined by x-ray diffraction for different parts of the ingots as well as thermograms analysis [8,9].

The thin films were prepared by conventional thermal evaporation under vacuum using silica crucible surrounded by a tungsten spiral filament and charged with the prepared ingots in granular form. The film was deposited onto glass and quartz substrates. In order to produce high quality with uniform thickness distribution S_xSe_{100-x} films a well-cleaned substrates were placed in a rotating holder with a rotation speed of about 240 rpm. The vacuum chamber was then pumped down to 10^{-4} Pa during deposition. The deposition rate was kept constant at 4 nm s^{-1} and the film thickness was controlled using a thickness monitor. The film thickness was measured after preparation by applying Tolansky's method [10]. After the preparation of the thin films the homogeneity was checked by repeating the optical measurements at least 5 times at different places for each sample. The structure of the compositions obtained was examined by energy dispersive x-ray spectrometry (EDX) and x-ray diffraction (XRD) as well as differential thermal analysis (DTA) techniques.

The transmittance, T , and reflectance, R , of the films deposited on quartz substrates were determined at normal incidence in the wavelength, range $\lambda = 400-2500 \text{ nm}$ by means of a double-beam spectrophotometer (JASCO 570)

attached to a specular reflection stage. If I_{fr} and I_q are the intensities of light passing through both the film-quartz system and the reference quartz respectively the experimental value of T is given as [11],

$$T_{exp} = (I_{fr} / I_q) (1 - R_q), \quad (1)$$

where R_q is the reflectance of quartz. Also, if the intensity of light reflected from the sample reaching the detector is I_{fr} and that reflected from reference aluminium mirror is I_{Al} , the experimental value of R is given as [12].

$$R_{exp} = (I_{fr} / I_{Al}) R_{Al} [1 + (1 - R_q)^2] - T^2 R_q \quad (2)$$

From the measured values of T_{exp} , R_{exp} and film thickness d , the values of the refractive index n , and the absorption index k , were computed by a special computer program [13] based on minimizing $(\Delta T)^2$ and $(\Delta R)^2$ simultaneously, where

$$(\Delta T)^2 = |T_{(n,k)} - T_{exp}|^2, \quad (3)$$

$$(\Delta R)^2 = |R_{(n,k)} - R_{exp}|^2, \quad (4)$$

where $T_{(n,k)}$ and $R_{(n,k)}$ are the values of T and R , calculated by using Murmann's exact equations [14,15]. By taking into account the experimental error in measuring the film thickness to be $\pm 2.6\%$ and in T_{exp} and R_{exp} to be $\pm 1\%$, the errors in the calculated values of n and k were estimated to be ± 3 and $\pm 2.5\%$, respectively.

3. Results and discussion

3.1. Optical constants

Three films of different thickness were prepared from each of the four compositions and the dependence of the transmittance, T , and reflectance, R , on the wavelength, λ , was obtained for each thickness. A representative example is given in Fig. 1 for sample with $x=7.28$ at % S having the thicknesses labeled on the curves. Interference bands are observed to the right of the absorption edge. The number of these bands across spectrum increases as the film thickness is increased. Figs. 2 and 3 represent the dispersion of n and the spectral distribution of k , respectively, which depend on the sulphur concentration. Fig. 2 represents the dispersion of n for samples containing 7.28 at % S. The curve, (a) is obtained before annealing and, (b), after annealing. In general, the dispersion curve has a peak in the vicinity of the absorption band at the wavelength which decreases with increasing sulphur content and shifts towards short wavelength. Fig. 3 shows the spectral distribution of k which depends on sulphur content. The change of n , and k , associated with the introduction of sulphur in the usual manner has a direct relation to the amount and strength of the different formed bonds in the network structure of the investigated compositions [8]. The parent glass Se (S at% = 0) of the system S_xSe_{1-x} has only one type of chemical bond namely the Se-Se in the three dimensional network structure. The

presence of S atoms instead of Se atoms leads to the replacement of Se-Se bonds by S-Se bonds [9]. By increasing the S content in selenium sample, the concentration of S-Se bonds increases on the expense of Se-Se bonds, and this leads to the decrease in the values of the optical constant n , and k as shown in Figs. 2, 3.

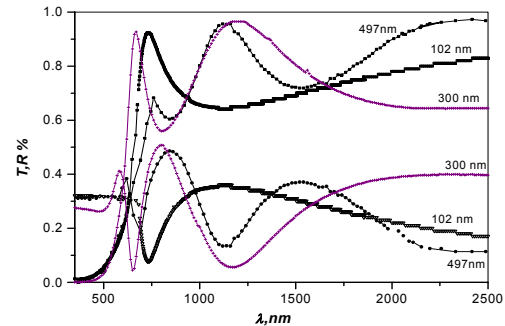


Fig. 1. Spectral distribution of the absolute values of the transmission, T , and reflection, R , of S_xSe_{1-x} Thin Films of Different Thicknesses, a) $x = 0$ at % S, b) $x = 2.5$ at % S, c) $x = 5.8$ at % S, d) $x = 7.28$ at % S.

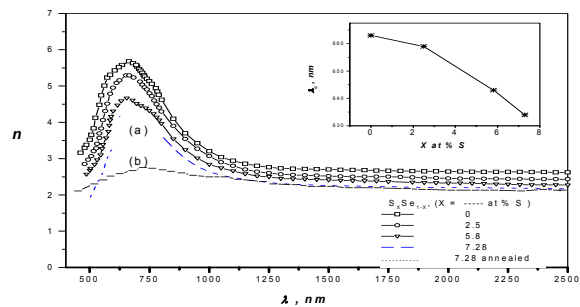


Fig. 2. Spectral distribution of the refractive index, n , for S_xSe_{1-x} thin films, $x = 0, 2.5, 5.8$ and 7.28 at % S.

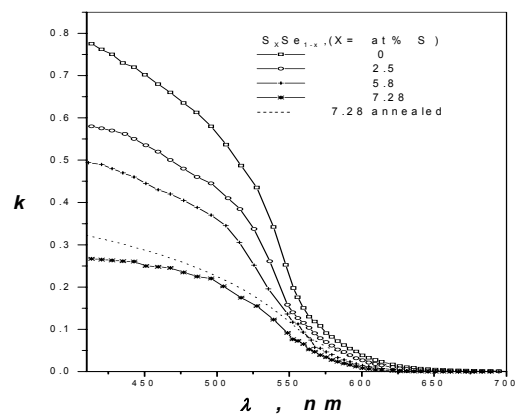


Fig. 3. Spectral distribution of the absorption index, k , for S_xSe_{1-x} thin films, $x = 0, 2.5, 5.8$ and 7.28 at % S.

3.2. Energy gap

The type of transition between valence band and conduction band can be identified from the relation between log(α) and log(hv) given in Fig. 4 for the tested compositions, where α is the absorption coefficient ($\alpha = 4 \pi k/\lambda$). As shown in Fig. 4, each curve, regardless the value of x, exhibits three different regions starting with a tail followed by two straight lines. These regions point to three different expected transitions. For the first region where the photon energy $h\nu < 1.80$ eV, the observed exponential absorption tail, obeys the Urbach tail [16]. In this photon energy range the absorption coefficient α , varies exponentially with the photon energy according to the empirical formula

$$\alpha = \alpha_0 \exp (h\nu/E_c) \tag{5}$$

where E_c is the Urbach parameter which often represents the width of localized state in the forbidden gap, and in general, represents the degree of disorder in amorphous semiconductors [17]. E_c was determined by plotting log α as a function of $h\nu$ as shown in Fig. 5. The determined values of E_c are given in Table 1. E_c decreases from 98 meV to 24.9 meV as the sulphur concentration increases from zero up to 7.28 at.%. This behaviour indicates a decrease in the degree of disorder [18] due to increasing sulphur content in the selenium matrix.

Table 1. Data analysis of the three regions of fig.: Urbach parameters, indirect energies and direct energy gap for each sulphur content in Se-S.

x, at %S	E_c , meV	$(\alpha h\nu)^{1/2}$	E_g^{ind} , eV $(\alpha/h\nu)^{1/2}$	$(h\nu \epsilon_2)^{1/2}$	E_{avg}^{ind} , eV	E_g^{ind} , eV as deposited	E_g^{ind} , eV annealed
0	98	1.845	1.838	1.84	1.8407	2.316	2.04
2.5	59.12	1.92	1.907	1.907	1.911	2.314	2.41
5.8	41.3	1.96	1.94	5.853	1.931	2.317	2.412
7.28	24.9	2.02	1.99	6.02	2.006	2.318	2.407

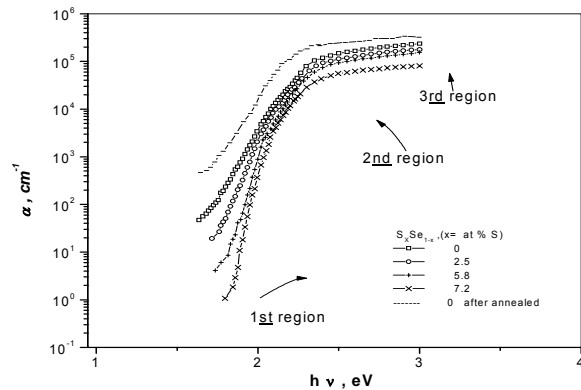


Fig. 4. Spectral behaviour of absorption coefficient, α versus the photon energy.

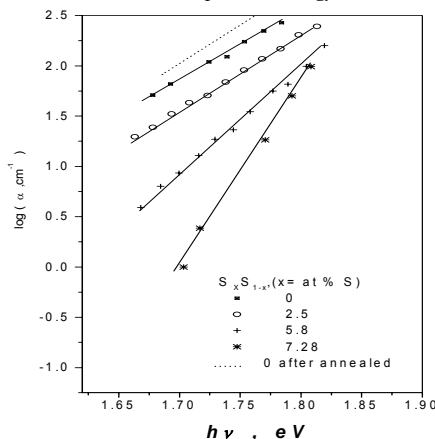


Fig. 5. Plot of Log (α) Versus ($h\nu$).

For photon energy in the range (1.8-2.25) eV, the optical energy gap and the type of transition were obtained for samples with different sulphur content by using the relation [19]

$$\alpha h\nu = A_0 (h\nu - E_g)^2 \tag{6}$$

Where A_0 is a constant. The optical energy gap calculated from the linear extrapolation of the plots of $(\alpha h\nu)^{1/2}$ vs. $h\nu$ to the energy axis for all compositions is given in Table 1. Applying the equations [20,21] of the forms

$$\alpha / h\nu = B_0 (h\nu - E_g)^2 \tag{7}$$

and

$$h\nu(\epsilon_2)^{1/2} = C_0 (h\nu - E_g) \tag{8}$$

and following the same procedure for expression, 6, the plots of both $(\alpha / h\nu)^{1/2}$ and/or $h\nu(\epsilon_2)^{1/2}$ vs. $h\nu$. The values of E_g obtained are given for comparison in Table 1. The similar values of E_g^{ind} due to the expressions, 6-8, ensure the existence of an indirect optical transition in this photon energy range and favor using the average indirect energy gap given in Table 1 for each composition of the S-Se system. The observed increase of the average E_g^{ind} with increasing Sulphur content can be explained as follows. The structure of the amorphous S - Se system is supposed to be that of equilibrium mixtures of linear polymer chains and eight-membered monomer rings [22]. Selenium consists of 40% monomers while monomer concentration in sulphur is 60%. As in the case of single component systems, the equilibrium copolymerization theory [23] developed for the liquid structure suggests that

copolymer molecules are in dynamic equilibrium with S_8 and Se_8 monomer molecules. In such a system the relative monomer-polymer concentrations are not only dependent on temperature, as in the single component systems, but also on the relative S and Se concentrations. Accordingly, the increase of the indirect energy gap (E_g^{ind}) by the addition of S up to 7.28 at.% to selenium is attributed to the concentration of monomer rings and the formation of S-Se bonds of greater strength than that of Se-Se bonds.

For the photon energy >2.25 eV, the straight lines relating $(\alpha h\nu)^2$ and $(h\nu)$ indicate a dominating direct allowed transition with direct energy gap, E_g^d , independent of sulphur content, as given in Table 1.

3.3. Dielectric constant

The relation between the refractive index, n and the oscillator strength below the band gap is given by the expression [24]:

$$n^2 - 1 = (E_d E_o) / (E_o^2 - E^2) \quad (9)$$

where E_o is the energy of the effective dispersion oscillator, E the photon energy, and E_d is the so-called dispersion energy which measures the average strength of the interband optical transitions. Fig. 6 shows the linear relation between $1/(n^2-1)$ and the square of the photon energy $(h\nu)^2$ for the investigated compositions. The values of E_d , E_o and ϵ_{∞} as determined from the slope and the intersection of the straight lines with $1/(n^2-1)$ axis are listed in Table 2. Both E_o and E_d increases while ϵ_{∞} decreases with increasing of the concentration of S in the investigated composition.

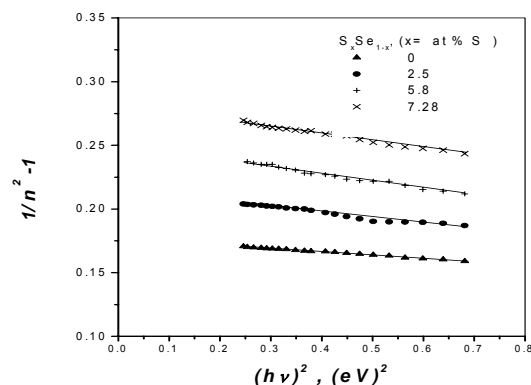


Fig. 6. Plot of $(1/n^2-1)$ versus $(h\nu)^2$ for as deposited S_xSe_{1-x} films.

The relation between the optical dielectric constant ϵ , wavelength λ and refractive index, n , is given by the equation [25]

$$\epsilon = n^2 = \epsilon_L - B\lambda^2 \quad (10)$$

where ϵ_L is the lattice dielectric constant and B is a constant equals $[N/4\pi c^2 \epsilon_o m^*]$ [26] and, depends on the ratio of carrier concentration to the effective mass N/m^* . Fig. 7 shows the relation between n^2 and λ^2 for the investigated compositions. Extrapolating the lines of Fig. 7 towards $\lambda^2 = 0$, the intercept at n^2 axis yields the value of ϵ_L , which decreases with increasing s content. From the slope, N/m^* can be obtained. The values calculated from Fig. 7 are given in Table 2. It is clear that increasing sulphur content increases the dispersion parameters and the indirect energy gap, while it decreases the ratio N/m^* , due to the increase of scattering centres by dissolution of the S atoms in the Se matrix [24].

Table 2. Dispersion parameters for S-Se films having different sulphur content.

x , at%S	λ_c , nm	n_{max}	E_o , eV	E_d , eV	ϵ_{∞}	ϵ_1	N/m^* , 1/gm.cm ⁻³
0	663	5.55	1.84	5.973	6.679	7.5059	1.14×10^{46}
2.5	659	5.31	1.86	6.706	5.656	6.63966	9.97×10^{46}
5.8	642	4.65	2.04	8.8048	4.834	6.21596	9.11×10^{46}
7.28	633	4.42	2.38	12.639	4.5395	5.24924	4.08×10^{46}
annealed							
7.28	630	4.36	2.4	10.51	4.78	5.91	7.08×10^{46}

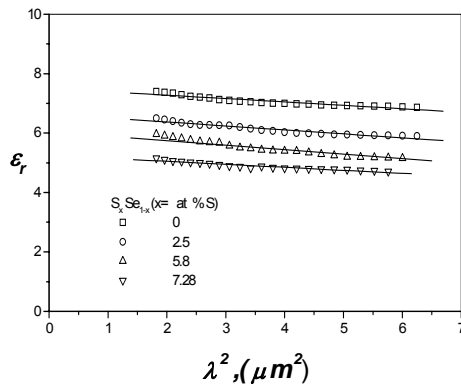


Fig. 7. Plot of n^2 versus λ^2 for as deposited S_xSe_{1-x} films.

3.3. Effect of heat treatment

The annealed samples were annealed at 423 K for 2h. The optical constants (n , k and α) were determined for the annealed films by using the same procedure as for the unannealed samples. As representative examples for the annealed samples, the curve for the relation, n vs. λ , was introduced in Fig. 2 for $x = 7.28$ at % S, for the relation, k vs. λ , with $x = 0$, was added to Fig. 3, and a curve for, α vs. $h\nu$, and $\log \alpha$ vs. $h\nu$ with $x=0$, was added to Fig. 4 and 5, respectively. The obtained parameters for the annealed samples were cited at the tables of the unannealed samples. The value of n found to decrease, Fig. 2 and both k , Fig. 3, and α , Figs. 4 and for 5, increased by the annealing process. The increase of the absorption coefficient, α , can be attributed to the high transition probability of the carriers [27]. The refractive index has the same behaviour of the as deposited film, Fig. 2. The width of the anomalous regions of the annealed samples is smaller than those for the as deposited films, and the peak of n was shifted towards shorter λ as the sulphur content was increased.

The obtained data from the relation of $(\alpha h\nu)^{1/2}$ as a function of $h\nu$ for the annealed thin films given in Table 1, as 2.14 show that the allowed indirect transitions still occur and the absorption edge is shifted to higher photon energy. The width of Urbach's tail is decreased by

annealing and nearly disappears for $x = 0$ (Se). The annealing tends to decrease the width of the tails of the localized states E_c and consequently decreases the disorder of the film [18]. The indirect optical gap is increased from 1.841 to 2.14 eV, Table 1, by increasing the sulphur content up to 7.28 at.% .

For the annealed films the values of the direct energy gap is still independent on sulphur content. This means that annealing at 433 K, reserves the persistent structure of the direct allowed transition but it leads to a small general increase in their values. The variation of the optical gap with S content can be represented by the following empirical relation for the as deposited thin films

$$E_g^{\text{ind}} (\text{as deposited films}) \approx 1.8420 + 0.027 x \quad (11)$$

where x represents the content of sulphur, while the variation of the optical gap with increasing sulphur can be represented by the following relation for the annealed thin films.

$$E_g^{\text{ind}} (\text{annealed films}) \approx 1.912 + 0.032 x. \quad (12)$$

The dispersion parameters of the annealed films are listed in Table 3. The increase of the values of the indirect optical energy gap of the investigated compositions by both annealing and increasing the sulphur content are discussed on the basis of Mott and Davis model [28]. The saturated bonds in amorphous semiconductors are responsible for the formation of the same defects in the materials. Such defects produce localized states in the band gap near the mobility edge. As the sulphur content increases in the examined composition, the increase of defects and the density of the localized states becomes responsible for the low values of the optical gap in case of the as deposited S-Se thin films. During the process of annealing the saturated defects gradually disappear and therefore [29] the reduction in the number of the unsaturated defects tends to decrease the density of the localized states in the band gap and consequently increase the optical gap.

Table 3. Dispersion parameters of the annealed S-Se films containing different sulphur contentent.

x , at%S	E_o , eV	E_d , eV	ϵ_∞	ϵ_1	N/m^3 , 1/gm.cm ⁻³
0	3.988	22.17	6.86	7.81	4.0719×10^{47}
2.5	4.128	23.43	6.75	7.71	3.97×10^{47}
5.8	4.236	24.4	6.68	7.63	2.647×10^{47}
7.28	4.359	25.5	6.57	7.52	2.31×10^{47}

4. Conclusions

Influence of sulphur content on the optical constants of the S_xSe_{100-x} thin films, where $x = 0, 2.5, 5.8$ and 7.28 at % S has been investigated. The obtained values of both n and k were found to be independent of the film thickness in the rang $100\text{-}500$ nm. The refractive index, n , attains a peak value at wavelength λ_c , which is shifted towards the shorter wavelength as the sulphur content is increased. This behaviour as explained by the presence of S atoms instead of Se atoms, leads to the replacement of Se-Se bonds by S-Se bonds. By increasing the S content, the concentration of S-Se bonds increases on the expense of Se-Se bonds, leading to the observed decrease in the values of the optical constants n , and k . The analysis of the spectral behaviour of absorption coefficient (α), in the absorption region revealed three different transitions. For the first region, where the photon energy obeys the Urbach's tail, decreases as the sulphur concentration increases. This behaviour indicates the decrease of disorder due to introducing of sulphur in selenium matrix. An indirect optical transition occurred in the second range where the value of optical gap increases as the S content increased. In the third region a direct allowed transition takes place. The values of the direct energy gap are independent on S content up to 7.28 at. % in the S-Se system.

The values of the dispersion energy E_d , the single oscillator energy E_0 , the infinite dielectric, the lattice dielectric constant and the ratio N/m^* , of the system have been determined. Both E_0 and E_d increase while ϵ_{∞} decreases with the increase of S content, in the investigated composition, n decreases with increasing S content, while decreases the ratio N/m^* decrease due to the increase of scattering centres by dissolution of the S atoms in the Se matrix. Annealing decreased both k and α coefficient can be attributed to the high transition probability of the carriers. The width of Urbach's tail is decreased by annealing and nearly disappears for Se. The indirect optical gap is increased by increasing the sulphur content up to 7.28 at.%. After annealing the values of the direct energy gap is still independent of the sulphur content. This means that annealing at 433 K, reserves the persistent structure of the direct allowed transition and leads to a small general increase in their values.

Acknowledgement

The authors are grateful to Prof. Dr. Fakhry abd El-Salam, Professor of physics, Faculty of Education, Ain Shams University, for fruitful discussions and great help.

References

- [1] S. R. Ovshinski, Phys. Rev. Letters, **21**, 1450 (1968).
- [2] J. Tauc "Proceedings of International Conference on the Physics of Semiconductors", Plenum Press, New York 159 (1974).
- [3] H. Frizche "proceedings of international conference on the physics of semiconductors", Plenum Press, New York, **221**, 313 (1974).
- [4] C. De Blasi, D. Manna, G. Miccoci, Tepore J. Appl. Phys. **63**, 1164 (1989).
- [5] V. Damodara Das, P. Jansi Lakshmi, J. Appl. Phys. **62**, 2376 (1987).
- [6] Y. Spripathi, G. B. Reddy, L. K. Malthora, J. Mater. Sci. Letters **2**, 109 (1991).
- [7] N. D. Baro, N. Clavaguera, S. Surinach, C. Barta, N. Rysava, A. Triska, J. Mater. Sci. **26**, 3680 (1991).
- [8] L. A. Wahab, M. B. El Den, M. S. Youssef, Egypt J. Sol. **32**, 1, 71 (2000).
- [9] Z. K. Heiba, M. B. El Den, Karimat El Sayed, J. Powder Diff. **17**, 3, 186 (2002).
- [10] S. Tolansky, "Multiple-beam Interference microscopy of metals". London: Academic Press, 55 (1970).
- [11] M. M. El-Nahas, J. Mater. Sci **27**, 6597 (1992).
- [12] Y. Laaziz, A. Bennouna, N. Chahboun, A. Outzourhit, thin solid films **372**, 149 (2000).
- [13] J. M. Bennet, M. J. Booty, Appl. Opt **5**, 41 (1966).
- [14] A. EL-Shazly, H. el-Shair, M. J. el-Nahas, Optics **12**(1), 6 (1983).
- [15] O. Z. Murman, Phys. **101**, 161 (1936).
- [16] A. Hruby, Stourac, Mat. Res. Bull, **6**, 465 (1971).
- [17] J. Schotmiller, M. Tabac, G. Lucovsky, J. Ward, No.Cryst.Solids, **4**, 80 (1970).
- [18] N. F. Mott, E. A. Davis, "Electronic processes in Non-crystalline materials" Clarendon press Oxford, ch:10(1971).
- [19] M. F. Kotkata, S. A. Nouh, L. Fakas, M. M. Radwan, J. Material. sci, **27**, 1785 (1992).
- [20] Set 31 of the powder diffraction file JCPDS.International center for diffraction Data :5 (8-247), se(6-0362) and ses (2- 032) 1998.
- [21] S. G. Tomlin, E. Khawaja. G. K. M. Thhutupalli, J. Phys. C: Solid State Phys. **9**, 4335 (1976). Pfister and Scher, Bull. Am. phys. Soc, 20 (1975).
- [22] M. B. Myers, E. J. Felty, Mat. Res. Bull. **2**, 535 (1967); Jauc J "Amorphous and liquid semiconductors", Plenum Press, New York 1974: 159.
- [23] A. Tobolsky, G. Owen, J. Polymer Sci. **59**, 329 (1962).
- [24] S. H. Wemple, M. Didomenico, phys. Rev. lett. **23**, 20, 1156 (1969).
- [25] W. G. Spitzer, J. M. Whelan, phys. Rev. **114**, 59 (1959).
- [26] G. A. Kumar, J. Thomas, N. George, B. A. Kumar, P. Radhokrishman, V. P. N. Nampoori, C. P. G. Vallabhan, J. Phys. Chem. Glasses **41**, 2, 89 (2000).
- [27] H. Kawazoc, H. Hosono, Leanazawa, J. Non-Crystalline Solids **29**, 159 (1975).
- [28] N. F. Mott, E. A. Davis "Electronic Processes in Non-Crystalline Materials", Clarendon Press, Oxford, Ch. 10, 1970.
- [29] H. T. EL-Shair, A. E. Bekheet, J. Phys. D: Appl. Phys. **25**, 1122 (1992).